HAL
open science

Carbonate system distribution, anthropogenic carbon and acidification in the western tropical South Pacific (OUTPACE 2015 transect)

Thibaut Wagener, Nicolas Metzl, Mathieu Caffin, Jonathan Fin, Sandra Helias Nunige, Dominique Lefèvre, Claire Lo Monaco, Gilles Rougier, Thierry Moutin

To cite this version:

Thibaut Wagener, Nicolas Metzl, Mathieu Caffin, Jonathan Fin, Sandra Helias Nunige, et al.. Carbonate system distribution, anthropogenic carbon and acidification in the western tropical South Pacific (OUTPACE 2015 transect). Biogeosciences, 2018, 15 (16), pp.5221 - 5236. 10.5194/bg-15-5221-2018 . hal-01868023

HAL Id: hal-01868023

https://hal.science/hal-01868023v1

Submitted on 5 Sep 2018

HAL is a multi-disciplinary open access archive for the deposit and dissemination of scientific research documents, whether they are published or not. The documents may come from teaching and research institutions in France or abroad, or from public or private research centers.

L'archive ouverte pluridisciplinaire **HAL**, est destinée au dépôt et à la diffusion de documents scientifiques de niveau recherche, publiés ou non, émanant des établissements d'enseignement et de recherche français ou étrangers, des laboratoires publics ou privés.

Biogeosciences, 15, 5221–5236, 2018
https://doi.org/10.5194/bg-15-5221-2018
© Author(s) 2018. This work is distributed under
the Creative Commons Attribution 4.0 License.

Biogeosciences
Open Access

Carbonate system distribution, anthropogenic carbon and acidification in the western tropical South Pacific (OUTPACE 2015 transect)

Thibaut Wagener[1], Nicolas Metzl[2], Mathieu Caffin[1], Jonathan Fin[2], Sandra Helias Nunige[1], Dominique Lefevre[1], Claire Lo Monaco[2], Gilles Rougier[1], and Thierry Moutin[1]

[1]Aix Marseille Univ, CNRS, IRD, Université de Toulon, MIO UM 110, 13288, Marseille, France
[2]Sorbonne Université, CNRS, IRD, MNHN, Laboratoire d'océanographie et du climat: expérimentation et approches numériques (LOCEAN), Case 100, 4 place Jussieu, 75252 Paris CEDEX 05, France

Correspondence: Thibaut Wagener (thibaut.wagener@univ-amu.fr)

Received: 9 April 2018 – Discussion started: 17 April 2018
Revised: 24 July 2018 – Accepted: 27 July 2018 – Published: 29 August 2018

Abstract. The western tropical South Pacific was sampled along a longitudinal 4000 km transect (OUTPACE cruise, 18 February, 3 April 2015) for the measurement of carbonate parameters (total alkalinity and total inorganic carbon) between the Melanesian Archipelago (MA) and the western part of the South Pacific gyre (WGY). This paper reports this new dataset and derived properties: pH on the total scale (pH_T) and the $CaCO_3$ saturation state with respect to aragonite (Ω_{ara}). We also estimate anthropogenic carbon (C_{ANT}) distribution in the water column using the TrOCA method (Tracer combining Oxygen, inorganic Carbon and total Alkalinity). Along the OUTPACE transect a deeper penetration of C_{ANT} in the intermediate waters was observed in the MA, whereas highest C_{ANT} concentrations were detected in the subsurface waters of the WGY. By combining our OUTPACE dataset with data available in GLODAPv2 (1974–2009), temporal changes in oceanic inorganic carbon were evaluated. An increase of 1.3 to 1.6 $\mu mol\,kg^{-1}\,a^{-1}$ for total inorganic carbon in the upper thermocline waters is estimated, whereas C_{ANT} increases by 1.1 to 1.2 $\mu mol\,kg^{-1}\,a^{-1}$. In the MA intermediate waters ($27\,kg\,m^{-3} < \sigma_\theta < 27.2\,kg\,m^{-3}$) an increase of 0.4 $\mu mol\,kg^{-1}\,a^{-1}$ C_{ANT} is detected. Our results suggest a clear progression of ocean acidification in the western tropical South Pacific with a decrease in the oceanic pH_T of up to $-0.0027\,a^{-1}$ and a shoaling of the saturation depth for aragonite of up to 200 m since the pre-industrial period.

1 Introduction

Human activities inject about 10 petagrams of carbon per year into the atmosphere, which might have major consequences on climate. It is recognized that the ocean plays a key role in the control of atmospheric CO_2 through uptake by the so-called "oceanic carbon pump". Through this "pump", the ocean sequesters ca. 25 % of the CO_2 injected annually into the atmosphere by human activities (Le Quéré et al., 2018). A consequence of the ocean carbon uptake is a decrease in the oceanic pH (Feely et al., 2004), which is described as ocean acidification (the so-called "other" CO_2 problem). Effects of ocean acidification have been observed in marine organisms and could affect the marine ecosystems (Riebesell et al., 2000). Improving our understanding of the oceanic CO_2 uptake relies primarily on observations of the marine carbonate cycle. Studies on the oceanic carbonate cycle have been mostly conducted in the framework of international programs. The World Ocean Circulation Experiment (WOCE) and the Joint Global Flux Study (JGOFS) in the 1990s coordinated oceanographic cruises along large sections in the ocean to collect samples through the water column and to perform accurate measurements of carbonate parameters and ancillary parameters (temperature, salinity, dissolved oxygen, nutrients, etc.). Since 2000, efforts have been made to revisit oceanic sections according to the WOCE strategy in order to assess oceanic changes at the scale of a decade. These programs have generated important databases

for oceanic carbonate chemistry (e.g., GLODAPv2, Olsen et al., 2016; Key et al., 2015).

In order to better assess the role of the ocean for the global carbon cycle, the concept of oceanic anthropogenic carbon (C_{ANT}) has been introduced and refers to the fraction of dissolved inorganic carbon (C_T) in the ocean that originates from carbon injected into the atmosphere by human activities since the industrial revolution. As C_{ANT} is not a directly measurable quantity, it can only be estimated through assumptions that are subject to intense scientific debate (Sabine and Tanhua, 2010). In particular, it has been recently recognized that ocean circulation changes drive significant variability in carbon uptake (DeVries et al., 2017). Detecting, separating and attributing decadal changes in the carbonate system (C_T and total alkalinity, A_T), C_{ANT} and pH in the ocean at global or regional scales remains challenging.

Within this context, the Pacific Ocean is a particularly challenging area to study due to its size (ca. one-third of the Earth's and one half of the oceanic surface). Even if, due to its remoteness from land, it remains largely underexplored by oceanographic vessels compared to other oceanic areas, the Pacific Ocean has been covered by cruises along long sections (the "P sections" from the WOCE program). Most of these sections have been revisited during the last years (e.g., Sabine et al., 2008; Kouketsu et al., 2013). In a recent study based on repeated sections in the Pacific (P16 at 150° W), Carter et al. (2017) observed a significant increase in C_{ANT} in the top 500 m around 10–30° S and a local carbon storage maximum around 20° S in recent years (between 2005 and 2014). In this context, the OUTPACE data presented in this study, associated with historical observations (since the pioneer 1974 GEOSECS, Geochemical Ocean Sections Program) offer a new view to evaluate variability and decadal changes in C_T, C_{ANT} and pH_T in the tropical Pacific, here focusing on the western tropical South Pacific (WTSP).

The aim of this paper is to report a new dataset of oceanic inorganic carbon (based on measurements of C_T and A_T) acquired in the WTSP during the OUTPACE (Oligotrophic to UltTra oligotrophic PACific Experiment) cruise performed in 2015 (Moutin et al., 2017). The main focus of the OUTPACE cruise was to study the complex interactions between planktonic organisms and the cycle of biogenic elements on different scales, motivated by the fact that the WTSP has been identified as a hot spot of N_2 fixation (Bonnet et al., 2017). The data presented here have been partially used in another paper of this special issue (Moutin et al., 2018) in order to study the biological carbon pump in the upper (surface to 200 m) water column. In this paper we will explore the carbonate data between the surface and 2000 m depth. The OUTPACE transect (Fig. 1) is close to existing WOCE and GO-SHIP (Global Ocean Ship-based Hydrographic Investigations Program) lines in the South Pacific: it is parallel to the zonal P21 line (18° S visited in 1994 and 2009) and the P06 line (32° S visited in 1992, 2003 and 2010), it is crossed by the meridional P14 line (180° E visited in 1994 and 2007) and P15 line (170° W visited in 2001, 2009 and 2016), and it is situated at the eastern side of the P16 line (150° W visited in 1992, 2005 and 2014). However, the OUTPACE transect does not correspond to any earlier occupation of the "WOCE lines" in the South Pacific and no tracers of water mass age were measured during the cruise, which limits the possibilities of a robust analysis of C_{ANT} accumulation in the area. Moreover, the horizontal and vertical resolution of the OUTPACE dataset is low. In consequence, the OUTPACE dataset cannot be used to look at decadal changes in C_{ANT} content in the South Pacific (e.g., Carter et al., 2017; Kouketsu et al., 2013). Here, C_{ANT} estimates based on the TrOCA (Tracer combining Oxygen, inorganic Carbon and total Alkalinity) method will be used as as a tool to investigate changes in C_T. Moreover, comparing our data with the high-quality data (internally consistent through a secondary quality control; Olsen et al., 2016) available in the Global Ocean Data analysis Project version 2 (GLODAPv2 database) will allow us to evaluate C_T, A_T, C_{ANT} (from TrOCA) and pH_T trends in subsurface waters and at depth.

The paper is organized as follows: after describing the methods used to acquire the dataset and the way the auxiliary data have been used in Sect. 2, we briefly present the hydrographic context of the cruise in Sect. 3. We then present in Sect. 4, the carbonate dataset acquired during the cruise. In Sect. 5, estimated C_{ANT} values in the water column are presented, the validity of these estimates based on the TrOCA method is discussed and geographical patterns are evoked. In Sect. 6, the temporal changes in oceanic inorganic carbon in the WTSP combining data available in GLODAPv2 and our OUTPACE dataset are presented and discussed. Finally, in Sect. 7, some features in relation to ocean acidification are inferred from our dataset.

2 Material and methods

2.1 Cruise and sampling strategy

The OUTPACE cruise took place between 18 February and 3 April 2015 from Nouméa (New Caledonia) to Papeete (French Polynesia), in the WTSP on board the French research vessel *L'Atalante* (Fig. 1). A total of 18 stations were sampled, mostly in the top 2000 m of the water column along a ∼ 4000 km transect from Melanesia to the South Pacific gyre (Moutin et al., 2017). A conductivity–temperature–depth (CTD) rosette was deployed to acquire data with CTD and associated sensors along vertical profiles and to collect discrete seawater samples from twenty-four 12 L Niskin bottles for chemical analysis. Due to technical failures on the main CTD rosette, for two of the casts considered in this study, a trace metal clean CTD rosette (TM-R) equipped with 24 teflon-lined GO-FLO bottles devoted to trace metal analyses was used. The configurations of both CTD rosettes are detailed elsewhere (Moutin et al., 2017).

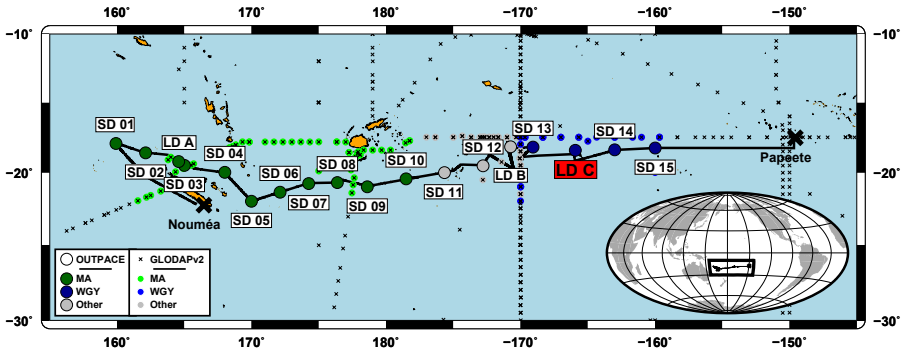

Figure 1. Map of the OUTPACE cruise transect. Melanesian Archipelago (MA) stations are indicated by large dark green large dots and the western gyre (WGY) stations by large dark blue dots. Stations outside of these two areas are in gray. The station in red corresponds to the station where the deep cast and intercomparison cast were made. Stations from the GLODAPv2 database are indicated with small crosses: small green dots correspond to GLODAPv2 stations considered for comparison in the MA area; small blue dots correspond to GLODAPv2 stations considered for comparison in the WGY area and small gray dots are the other GLODAPv2 stations considered for comparison.

For carbonate parameters, seawater was sampled from 37 casts over the 18 stations. At each station, on a regular basis, samples were collected at 12 depths between the surface and 2000 m on two distinct casts: six samples on a 0–200 m cast and six samples on a 0–2000 m cast. At station SD 13, only one cast was sampled down to 500 m depth. In addition, at station LD C, samples were collected at 24 depths on a deep cast (down to 5000 m) and 12 samples were collected at the same depth (25 m) on a "repeatability" cast. Details on the casts performed for this study are summarized in Table 1.

2.2 Chemical measurements on discrete samples

All samples were collected within less than 1 h after arrival of the CTD rosette on deck.

2.2.1 Total alkalinity and dissolved inorganic carbon

Samples for A_T and C_T were collected in one 500 mL borosilicate glass flask (Schott Duran®) and poisoned with $HgCl_2$ immediately after collection (final concentration 20 mg L^{-1}). Samples were stored at 4 °C during transport and were analyzed (within 10 days of each other) 5 months after the end of the cruise at the SNAPO-CO_2 (Service National d'Analyse des paramètres Océaniques du CO_2 – LOCEAN – Paris). A_T and C_T were measured on the same sample based on a potentiometric titration in a closed cell (Edmond, 1970). A nonlinear curve fitting approach was used to estimate A_T and C_T from the recorded titration data (Dickson, 1981; Dickson and Goyet, 1994). Measurements were calibrated with certified reference material (CRM) provided by Andrew Dickson, University of Southern California (batch 139 – C_T: 2023.23 ± 0.70 µmol kg^{-1} and A_T: 2250.82 ± 0.60 µmol kg^{-1}; see Dickson, 2010). The reproducibility, expressed as the standard deviation of the CRM analysis ($n = 15$), was 4.6 µmol kg^{-1} for A_T and 4.7 µmol kg^{-1} for C_T. Based on replicate measurements at station LD C (cast out_c_194; see Table 1), the reproducibility, expressed as the standard deviation of the analysis of the replicates collected at the same depth (ca. 25 m, $n = 12$) from different Niskin bottles, was 3.6 µmol kg^{-1} for A_T (average value : 2324.7 µmol kg^{-1}) and 3.7 µmol kg^{-1} for C_T (average value : 1969.7 µmol kg^{-1}).

2.2.2 Oxygen concentration

Dissolved oxygen concentration [O_2] was measured following the Winkler method (Winkler, 1888) with potentiometric endpoint detection (Oudot et al., 1988). For sampling, reagent preparation and analysis, the recommendations from Langdon (2010) were carefully followed. The thiosulfate solution was calibrated by titrating it against a potassium iodate certified standard solution of 0.0100 N (CSK standard solution – WAKO™). The reproducibility, expressed as the standard deviation of replicates samples was 0.8 µmol kg^{-1} ($n = 15$; average value : 195.4 µmol kg^{-1}).

2.3 Vertical profiles of hydrological and biogeochemical parameters

2.3.1 CTD measurements

CTD measurements were ensured by a Seabird™ 911+ underwater unit, which interfaced an internal pressure sensor, two redundant external temperature probes (SBE3plus) and two redundant external conductivity cells (SBE4C). The sensors were calibrated pre- and post-cruise by the manufacturer. No significant drift between the redundant sensors was observed. For vertical profiles, full-resolution data (24 Hz) were reduced to 1 dbar binned vertical profiles on the downcast with a suite of processing modules using the Seabird™ dedicated software (SbeDataProcessing). For values at the closure of the Niskin bottles, values collected at 24 Hz were averaged 3 s before and 5 s after closure of the bottle. In

Table 1. General description of the casts sampled for carbonate chemistry parameters during the OUTPACE cruise.

Cast	Station	Longitude (° E)	Latitude (° N)	Time (UTC)	Max. pres. (dbar)	Type[a]	Rosette[b]
out_c_006	SD 1	159.9255	−17.9418	2015/02/22 03:08:00	202	SHAW	CLA
out_t_002		159.9425	−17.9088	2015/02/22 07:43:00	2000	INT	TMC
out_c_010	SD 2	162.1248	−18.6078	2015/02/23 00:11:00	199	SHAW	CLA
out_c_016		162.1112	−18.5845	2015/02/23 08:16:00	1998	INT	CLA
out_c_019	SD 3	165.0093	−19.4955	2015/02/24 05:58:00	200	SHAW	CLA
out_c_020		165.0082	−19.4907	2015/02/24 08:14:00	1999	INT	CLA
out_c_066	LD A	164.5877	−19.2242	2015/03/02 14:39:00	200	SHAW	CLA
out_c_067		164.5787	−19.2233	2015/03/02 16:10:00	2002	INT	CLA
out_c_070	SD 4	168.0118	−19.9832	2015/03/04 10:55:00	201	SHAW	CLA
out_c_071		168.0157	−19.98	2015/03/04 12:43:00	1999	INT	CLA
out_c_074	SD 5	169.9943	−22.0002	2015/03/05 08:48:00	201	SHAW	CLA
out_c_075		169.9965	−21.9997	2015/03/05 10:27:00	1999	INT	CLA
out_c_078	SD 6	172.1198	−21.3732	2015/03/06 07:27:00	200	SHAW	CLA
out_c_079		172.1193	−21.3758	2015/03/06 09:08:00	1999	INT	CLA
out_c_082	SD 7	174.25	−20.7697	2015/03/07 05:09:00	201	SHAW	CLA
out_c_083		174.2512	−20.7677	2015/03/07 06:37:00	2000	INT	CLA
out_c_086	SD 8	176.3778	−20.7027	2015/03/08 02:31:00	201	SHAW	CLA
out_c_087		176.364	−20.6945	2015/03/08 04:19:00	1997	INT	CLA
out_c_091	SD 9	178.6087	−20.9963	2015/03/09 04:57:00	2002	INT	CLA
out_t_012		178.6062	−20.9892	2015/03/09 06:46:00	201	SHAW	TMC
out_c_094	SD 10	−178.5105	−20.4417	2015/03/10 04:10:00	200	SHAW	CLA
out_c_095		−178.5105	−20.44	2015/03/10 05:48:00	762	INT	CLA
out_c_098	SD 11	−175.6542	−20.0028	2015/03/11 00:53:00	207	SHAW	CLA
out_c_099		−175.6475	−20.0057	2015/03/11 02:46:00	2000	INT	CLA
out_c_102	SD 12	−172.7885	−19.5237	2015/03/12 00:38:00	200	SHAW	CLA
out_c_103		−172.7813	−19.5368	2015/03/12 02:26:00	2001	INT	CLA
out_c_150	LD B	−170.7433	−18.179	2015/03/20 12:38:00	204	SHAW	CLA
out_c_151		−170.7385	−18.1745	2015/03/20 14:16:00	1997	INT	CLA
out_c_152	SD 13	−169.0728	−18.2007	2015/03/21 10:27:00	501	INT	CLA
out_c_163		−165.9315	−18.4282	2015/03/24 12:23:00	5027	DEEP	CLA
out_c_194	LD C	−165.8647	−18.4952	2015/03/28 02:01:00	25	REPRO	CLA
out_c_198		−165.7915	−18.4912	2015/03/28 12:42:00	298	SHAW	CLA
out_c_199		−165.7792	−18.4842	2015/03/28 14:32:00	2001	INT	CLA
out_c_209	SD 14	−163.001	−18.395	2015/03/30 05:19:00	300	SHAW	CLA
out_c_210		−162.9992	−18.3952	2015/03/30 07:03:00	2000	INT	CLA
out_c_212	SD 15	−159.9913	−18.265	2015/03/31 04:01:00	300	SHAW	CLA
out_c_213		−159.9913	−18.2618	2015/03/31 05:41:00	2002	INT	CLA

[a] SHAW stands for casts up to 200 dbar, INT stands for casts up to 2000 dbar, DEEP stands for the deep cast and REPRO stands for the cast with reproducibility measurements. [b] A CTD was rosette used for the cast. CLA is the normal CTD rosette, and TMC is the trace metal clean rosette (see Sect. 2.1).

this study, for temperature and conductivity the signal of the first sensors has been used systematically. For the two TM-R casts, no significant difference with the main CTD rosette on temperature and conductivity was observed.

2.3.2 Oxygen measurements

$[O_2]$ was also measured with a SBE43 electrochemical sensor interfaced with the CTD unit. The raw voltage was converted to oxygen concentration with 13 calibration coefficients based on the Seabird™ methodology derived from Owens and Millard (1985). Three of these coefficients (the oxygen signal slope, the voltage at zero oxygen signal, the pressure correction factor) were adjusted with the concentrations estimated with the Winkler method on samples collected at the closure of the bottles. One unique set of calibration coefficients has been applied to all oxygen profiles from the cruise because no significant drift of the sensor was observed during the time of the cruise. For the two TM-R casts, values have been corrected with a drift and offset based on the comparison of 15 pairs of casts (main CTD rosette/TM-R) collected close in time (less than 2 h) and space (less than 1 nautical mile) over the entire OUTPACE transect.

2.4 Derived parameters

Practical salinity (S_P) was derived from conductivity, temperature and pressure with the EPS-78 algorithm. Absolute

salinity (S_A), potential temperature (θ), conservative temperature (Θ) and potential density (σ_θ) were derived from S_P, temperature, pressure and the geographic position with the TEOS-10 algorithms (Valladares et al., 2011). These five derived parameters were calculated within the processing with Seabird™ dedicated software.

Seawater pH on the total scale (pH_T) and the $CaCO_3$ saturation state with respect to aragonite (Ω_{ara}) were derived from A_T and C_T with the "Seacarb" R package (Gattuso and Lavigne, 2009). $CaCO_3$ saturation state with respect to calcite was not considered because seawater up to 2000 dbar was supersaturated with respect to calcite ($\Omega_{cal} > 1$). Following the recommendations from Dickson et al. (2007), the constants for carbonic acid K_1 and K_2 from Lueker et al. (2000), the constant for hydrogen fluoride K_F from Pérez and Fraga (1987), and the constant for hydrogen sulfate K_S from Dickson (1990) were used. Orthophosphate and silicate concentration were considered in the calculation. Methods for nutrient measurement are presented in detail in Fumenia et al. (2018). When nutrient data were not available (station SD 8), silicate and orthophosphate were estimated from the nutrient profile measured on cast out_c_163 (interpolated values). Apparent oxygen utilization (AOU) was computed from the difference between oxygen solubility (at $p = 0$ dbar, and S_P) estimated with the "Benson and Krause coefficients" in Garcia and Gordon (1992) and in situ $[O_2]$.

For the estimation of C_{ANT}, the TrOCA method was used. The TrOCA approach was first proposed in Touratier and Goyet (2004a, b) with improvements in Touratier et al. (2007). In brief, the TrOCA parameter is defined as a combination of A_T, C_T and $[O_2]$ that accounts for biologically induced relative changes among these parameters (with constant stoichiometric ratios). TrOCA is thus a quasi-conservative tracer derived from C_T in the ocean. Within a defined water mass, changes in TrOCA over time are independent of biology and can be attributed to the penetration of C_{ANT}. In consequence C_{ANT} can be calculated in a parcel of water from the difference between current and pre-industrial TrOCA (TrOCA°) divided by a stoichiometric coefficient. The simplicity of the TrOCA method relies on the fact that a simple formulation for TROCA° has been proposed based on potential temperature and alkalinity and thus an estimation of C_{ANT} can be done by a simple calculation using C_T, A_T, $[O_2]$ and θ. In this study, the formulation proposed in Eq. (11) in Touratier et al. (2007) is used to calculate C_{ANT} and is recalled here in Eq. (1).

$$C_{ANT} = \left([O_2] + 1.279\left(C_T - \frac{A_T}{2}\right) - \exp\left(7.511 - 1.087\times10^{-2}\,\theta - \frac{7.81\times10^{-5}}{A_T^2}\right)\right)\Big/1.279 \quad (1)$$

This formulation is based on an adjustment of the TrOCA coefficients using $\Delta^{14}C$ and CFC-11 from the GLODAPv1 database (Key et al., 2004). Touratier et al. (2007) estimated the overall uncertainty of the C_{ANT} with TrOCA method to be ca. 6 µmol kg^{-1} based on the random propagation of the uncertainties in the variables (C_T, A_T, $[O_2]$ and θ) and coefficients used in Eq. (1). The limitations and validity of the TrOCA method will be discussed in detail in Sect. 5.

2.5 Data from available databases

For comparison with existing values of carbonate chemistry in the area of the OUTPACE cruise, relevant data were extracted from GLODAPv2 database (NDP-93 – Olsen et al., 2016; Key et al., 2015). The specific data file for the Pacific Ocean was used (downloaded from https://www.nodc.noaa.gov/ocads/oceans/GLODAPv2/, last access: 14 December 2017). For comparison with OUTPACE data, GLODAPv2 data were selected between 22 and 17° S and between 159° E and 159° W (going westwards). For specific comparisons in the MA and the South Pacific western gyre waters (WGY) a zonal subset of the extracted data was used: 159° E and 178° W for MA and 170 to 159° W for WGY (see Fig. 1).

3 Hydrological context along the OUTPACE transect

The hydrological context encountered during the OUTPACE transect is presented with a $\Theta - S_A$ diagram between 0 and 2000 dbar in Fig. 2. A detailed description of the water masses encountered during the OUTPACE cruise can be found in Fumenia et al. (2018). Briefly, from the surface to 2000 dbar, the following features are distinguished: the surface waters ($\sigma_\theta < 23.5$ kg m^{-3}) were characterized by temperatures over 25 °C with increasing temperature and salinity towards the east and AOU close to zero. Under the surface water, the upper thermocline waters (UTW) presented a maximum in salinity, reaching values higher than 36 g kg^{-1} in the eastern part of the cruise. In the lower thermocline waters, S_A decreased with depth with a more pronounced decrease in the eastern part than in the western part, whereas AOU is higher in the eastern part than in the western part of the studied area. These differences in lower thermocline waters have been described for South Pacific Central Waters (SPCW) with more saline western (WSPCW) and less saline eastern (ESPCW) waters (Tomczak and Godfrey, 2003). Below the thermocline, intermediate waters are made up of Subantarctic Mode Waters (SAMW) and Antarctic Intermediate Waters (AAIWs). AAIWs have a salinity minimum close to the $\sigma_\theta = 27$ kg m^{-3} isopycnal. Hartin et al. (2011) defines SAMW as having σ_θ values between 26.80 and 27.06 kg m^{-3}, corresponding to a minimum in potential vorticity, and AAIW as having σ_θ values between 27.06 and 27.40 kg m^{-3}. The separation of both waters is not trivial in the subtropical area.

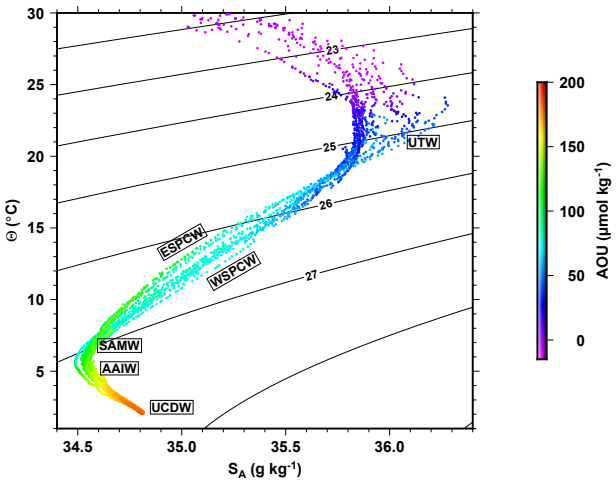

Figure 2. $\Theta - S_A$ diagram with colors indicating the AOU. Black contour lines represent the isopycnal horizons based on potential density referenced to a pressure of 0 dbar (σ_θ).

SAMW is generally associated with lower AOU than AAIW. Finally, deep waters made up of Upper Circumpolar Deep Waters (UCDW) correspond to an increase in salinity and AOU for depth corresponding to $\sigma_\theta > 27.4\,\mathrm{kg\,m^{-3}}$.

In this study, discussion will sometimes make a distinction between two subregions along the OUTPACE transect: MA and WGY (see Sect. 2.5 for definition). This distinction is mainly based on geographic and oceanographic arguments. Indeed, these two subregions are geographically separated by the Tonga volcanic arc. WGY is characterized by higher surface temperature and a higher salinity in the upper thermocline waters than MA. The difference between these subregions is evidenced by the difference in oligotrophy (Moutin et al., 2018). Due to specific conditions in the transition area between the MA and WGY (de Verneil et al., 2017), SD 11, SD 12 and LD B were discarded from both groups in this study following the arguments in Moutin et al. (2018).

4 Carbonate chemistry along the OUTPACE transect

A_T and C_T measured along the OUTPACE transect are presented in Fig. 3a and b. All vertical profiles for A_T, A_T normalized to $S_A = 35\,\mathrm{g\,kg^{-1}}$ ($A_{T\,n35}$) and C_T are presented in Fig. 3e, f and g. A_T ranged between 2300 and 2400 µmol kg^{-1}. Below the surface, a pronounced maximum in A_T was observed associated with the saltier upper thermocline waters. When normalized to $S_A = 35\,\mathrm{g\,kg^{-1}}$, $A_{T\,n35}$ values are remarkably constant in the upper 500 dbar with values between 2270 and 2310 µmol kg^{-1}. Below 500 dbar, A_T increases with depth up to ca. 2400 µmol kg^{-1} indicating that alkalinity changes are mostly due to salinity changes in the upper water column, whereas the increase in the deep waters is mainly due to carbonate biomineral remineralization. C_T values are close to 1950 µmol kg^{-1} in the surface and increase with depth up to 2300 µmol kg^{-1} at 2000 dbar. The C_T gradient in the upper water column has been described in Moutin et al. (2018). Below 2000 dbar, C_T is relatively invariant with slightly lower values in the bottom waters (below 4000 dbar) due to the presence of very old deep waters originating from the North Pacific relative to the northward moving bottom waters that have not accumulated as much carbon (Murata et al., 2007). A_T and C_T values in deep waters measured during OUTPACE are in good agreement with the data of the GLODAPv2 database (Fig. 3e, f and g). No systematic adjustment of the OUTPACE dataset with the GLODAPv2 dataset was performed because only very few data are available in the deep ocean where crossover comparison can be performed for cruises carried out in different decades. Nevertheless, for the only "deep" cast performed during OUTPACE (out_c_163 at station LD C), we performed a simple crossover analysis with the station 189 (located at 107 km kilometers from OUTPACE station LD C) of the Japanese "P21 revisited" cruise in 2009. We compared interpolated profiles on density surfaces values ($27.75\,\mathrm{kg\,m^{-3}} < \sigma_\theta < 27.83\,\mathrm{kg\,m^{-1}}$ corresponding to pressure levels of ca. 3000 to 5500 dbar). The estimated offsets are -2.0 ± 4.2 µmol kg^{-1} for A_T and -2.0 ± 4.4 µmol kg^{-1} for C_T suggesting measurement biases are likely no larger. This simple quality control procedure seems to indicate that no systematic adjustment is needed.

Derived parameters from the A_T and C_T measurements are presented in Fig. 3c for pH_T values (estimated at in situ temperature and pressure). pH_T decreases from values close to 8.06 in surface to values close to 7.84 at 2000 m. Surface values of pH_T are typical of subtropical warm waters and are in a similar range as the austral summer values estimated by Takahashi et al. (2014) in this area (8.06–8.08). Figure 3d represents the vertical distribution of computed values of Ω_{ara} along the OUTPACE transect. Seawater is supersaturated with respect to aragonite ($\Omega_{ara} > 1$) at the surface with Ω_{ara} values of ca. 4.0 again in good agreement with the austral summer values of 4–4.4 estimated by Takahashi et al. (2014) in this area. Values of Ω_{ara} decrease with depth, and seawater becomes undersaturated with respect to aragonite ($\Omega_{ara} < 1$) at an horizon situated below 1000 dbar in the west and above 1000 dbar in the eastern part of the cruise, with a general shoaling of the Ω_{ara} values from west to east, in good agreement with a previous study by Murata et al. (2015) in this area.

5 Anthropogenic carbon estimation along the OUTPACE transect

The TrOCA method is a way to quantify C_{ANT} in the ocean based on C_T, A_T, $[O_2]$ and θ. This method has been used and compared to other methods in different oceanic areas (e.g., Lo Monaco et al., 2005; Álvarez et al., 2009;

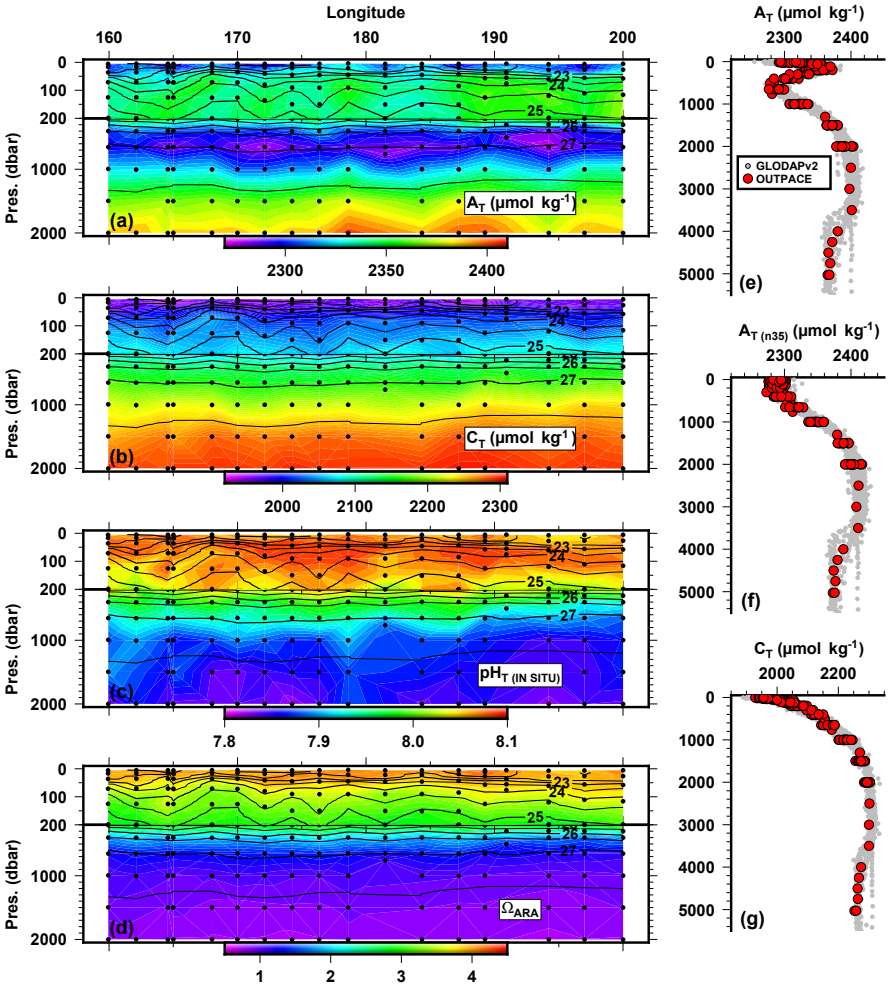

Figure 3. Longitudinal variations in **(a)** A_T, **(b)** C_T, **(c)** pH_T and **(d)** Ω_{ara} along the OUTPACE transect between the surface and 2000 dbar depth. Black contour lines represent the isopycnal horizons based on potential density referenced to a pressure of 0 dbar. Vertical profiles of **(e)** A_T, **(f)** $A_{T\ n35}$ and **(g)** C_T of the entire OUTPACE dataset (red dots) superimposed on the GLODAPv2 data corresponding to the OUTPACE area (gray dots).

Vázquez-Rodríguez et al., 2009). Based on specific C_{ANT} inventories in the water column, the TrOCA method reasonably agreed with the other methods (including the transient tracer-based method). However, Yool et al. (2010) "tested" the TrOCA method within an ocean general circulation model and argued that the use of globally uniform parameterization for the estimation of the pre-industrial TrOCA is a source of significant overestimation but also that even with regionally "tuned" parameters a global positive bias in the method exists. As no tracers of water mass age were measured during the OUTPACE cruise, the main motivation for using the TrOCA method was to make C_{ANT} estimations based on a simple calculation from parameters acquired within the cruise as done in other cruises conducted in tropical South Pacific waters (e.g., Azouzi et al., 2009; Ganachaud et al., 2017). Even if C_{ANT} estimates from TrOCA are biased, the application of a simple back-calculation method that accounts for biologically induced relative changes in C_T is used here to identify some spatial features in the distribution of the carbonate system along the OUTPACE transect. Here, an error in the TrOCA C_{ANT} estimates of 67 % will be considered based on the standard deviation for the TrOCA variant optimized with world ocean data and normalized such that standard deviation in the simulated C_{ANT} in the ocean general circulation model is exactly 1 (see Table 2 in Yool et al., 2010).

As mentioned by Touratier et al. (2007), C_{ANT} estimates cannot be considered within the mixed layer because the underlying hypotheses used in the formulation of TrOCA may not be verified due to biological activity and gas transfers across the air–sea interface. To avoid this issue, C_{ANT} estimates are generally used below the "permanent" mixed layer depth (e.g., Álvarez et al., 2009; Carter et al., 2017). For the OUTPACE area, Moutin et al. (2018) show that the mixed

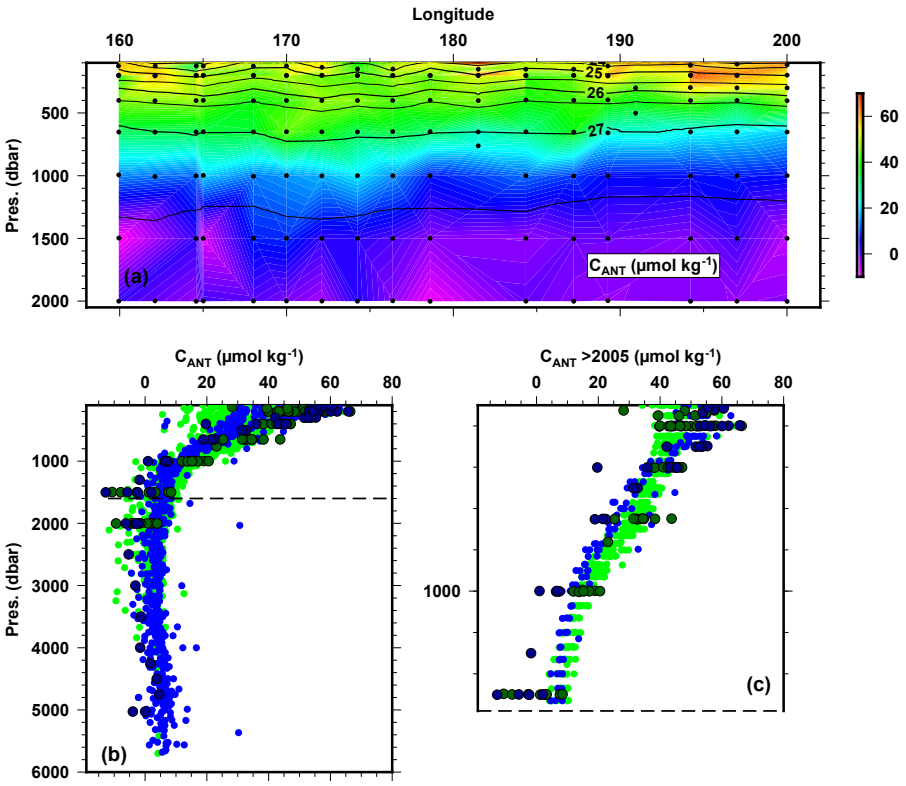

Figure 4. Longitudinal variations in C_{ANT} (estimated with the TrOCA method) along the OUTPACE transect between 100 and 2000 dbar depth **(a)**. Black contour lines represents the isopycnal horizons based on potential density referenced to a pressure of 0 dbar. Vertical profiles of C_{ANT} for the entire OUTPACE dataset superimposed on the values estimated from the GLODAPv2 data **(b)** and vertical profiles of C_{ANT} between 100 and 1500 dbar superimposed on the values estimated from the recent (after 2005) GLODAPv2 data **(c)**. The color code for the dots is the same as for Fig. 1.

layer depth does not exceed 70 m in the area. Even if the depths of the deep chlorophyll maximum were encountered below 100 dbar along the transect, we will consider C_{ANT} values up to 100 dbar. It can be mentioned that the C_{ANT} values of 50–60 µmol kg^{-1} in the top of the water column (100 dbar) are in reasonable agreement with a rough estimate of thermodynamically consistent C_T changes: by assuming that CO_2 in surface seawater is in equilibrium with the atmosphere, we estimated that with a partial pressure of CO_2 (pCO_2) of 280 µatm in the pre-industrial period, a pCO_2 of 380 µatm during OUTPACE (Moutin et al., 2018) and a constant A_T over time of 2300 µmol kg^{-1}, C_T change in surface waters between the pre-industrial period and 2015 is ca. 65 µmol kg^{-1} for a temperature of surface waters between 25 and 28 °C. For OUTPACE, C_{ANT} estimates below 1000 dbar were not significantly different from 0 µmol kg^{-1}, with a standard deviation of 6.3 µmol kg^{-1}.

C_{ANT} distribution along the OUTPACE transect is presented in Fig. 4a, and all vertical profiles for C_{ANT} are presented in Fig. 4b with a more detailed view of the first 1500 dbar of the water column in Fig. 4c. Figure 4b and c distinguish values from the MA and the WGY area. The C_{ANT} vertical profiles suggest a penetration of anthropogenic carbon up to 1000 dbar. As mentioned before, estimated values of C_{ANT} reach values of 60 ± 40 µmol kg^{-1} at a depth of 100 dbar; C_{ANT} then regularly decreases to values close to 10–20 $\pm$ 13 µmol kg^{-1} at a depth of 1000 dbar and reaches values close to 0 µmol kg^{-1} below 1500 dbar. The zonal C_{ANT} section along the OUTPACE transect (Fig. 4a) presents two features: (1) a deeper penetration of C_{ANT} in the western part of the transect with values of C_{ANT} reaching 40 ± 25 µmol kg^{-1} around the isopycnal layer of 27 kg m^{-3} (ca. 700 dbar) with a coherent behavior with the distribution of AOU and (2) a larger accumulation of C_{ANT} in the eastern part of the transect centered around the isopycnal layer of 25 kg m^{-3} (ca. 200 dbar).

Several studies have identified deeper C_{ANT} penetration in the western South Pacific than in the eastern South Pacific at tropical and subtropical latitudes. The primary reason for this longitudinal difference might be associated with deeper convection in the western part and upwelling in the eastern part. AAIW has been described as the lower limit of the penetration of C_{ANT} in the ocean interior of the South Pacific (Sabine et al., 2004). Moreover, a recent study by

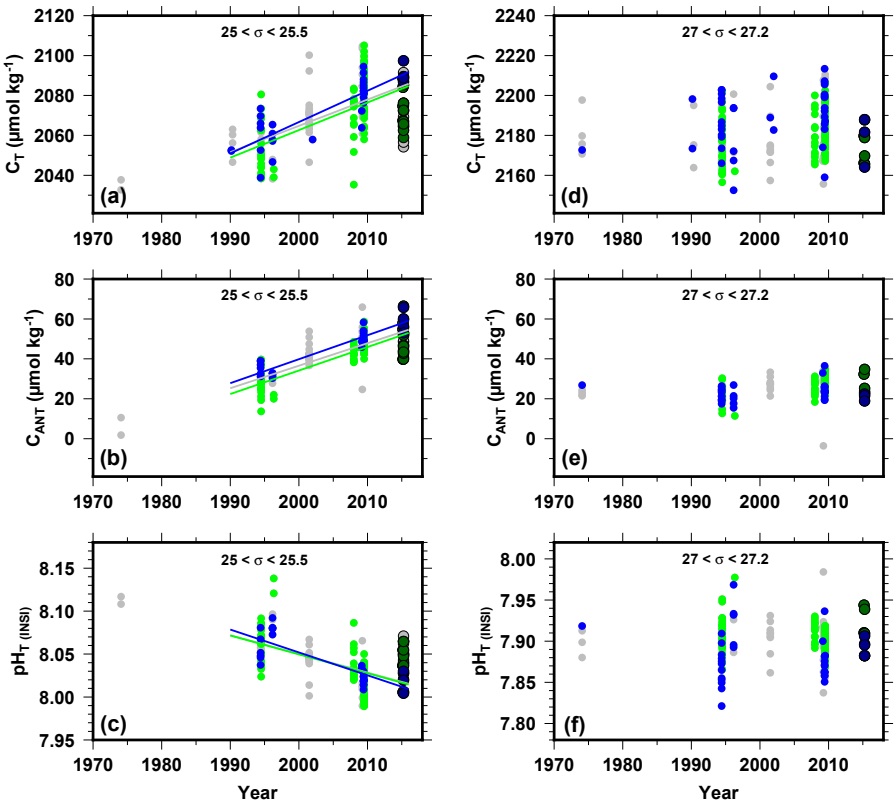

Figure 5. Temporal evolution in the OUTPACE area of C_T **(a, d)**, C_{ANT} **(b, e)** and pH_{Tinsi} **(c, f)** based on GLODAPv2 and OUTPACE data along two isopycnal layers: 25–25.5 kg m^{-3} **(a, b, c)** and 27–27.2 kg m^{-3} **(d, e, f)**. The color code for the dots is the same as for Fig. 1.

DeVries et al. (2017) shows that ocean circulation variability is the primary driver for changes in oceanic CO_2 uptake at decadal scales. Based on C_T changes between the two repeated visits of the longitudinal P21 line (18° S close to the OUTPACE transect) in 1994 and 2009, Kouketsu et al. (2013) show a faster increase in C_{ANT} in the western part than in the eastern part of the section. They also postulate that C_{ANT} may have been transported by deep circulation associated with the AAIW. In the subtropical Pacific along the P06 line (longitudinal section at ca. 32° S), Murata et al. (2007) also identified an increase in C_{ANT} in the SAMW and AAIW. Waters et al. (2011) attribute the deeper penetration of C_{ANT} in the western part of the section to the local formation of subtropical mode water in the area based on the extended multiple linear regression (eMLR) method along the P06 line (and taking into account a third visit).

In the eastern part of the OUTPACE cruise, the detected accumulation of C_{ANT} in the upper thermocline waters may be related to recent observations of a significant accumulation of C_{ANT} at latitudes around 20° S on the P16 meridional transect along 150° W by Carter et al. (2017). This change in C_{ANT} accumulation is attributed to changes in the degree of the water mass ventilation due to variability in a southern Pacific subtropical cell. Along the P16 line, Carter et al. (2017) observed high values of C_{ANT} (up to 60 µmol kg^{-1}) for the upper water column at the latitude of the OUTPACE area in good agreement with our estimates in WGY in the upper water column. Finally, it should also be mentioned that, due to the presence of one of the main oxygen minimum zone (OMZ) area, denitrification occurs in the eastern South Pacific and can be traced by the N^* parameter (Gruber and Sarmiento, 1997). Denitrification, by transforming organic carbon to inorganic carbon without the consumption of oxygen, could induce an overestimation of C_{ANT} by the TrOCA method (and other back-calculation methods) due to a biological release of C_T that is not taken into account in the formulation of the quasi-conservative TrOCA tracer. Horizontal advection by the south equatorial current of the strong negative N^* signal originating from the eastern Pacific towards the western Pacific has been described previously (Yoshikawa et al., 2015). Fumenia et al. (2018) have estimated N^* along the OUTPACE transect and show slightly negative N^* values in the upper thermocline waters at the eastern side of the OUTPACE transect where the highest C_{ANT} values are estimated. However, Murata et al. (2015) showed that, based on a direct relation between C_T and N^*, the influence of denitrification should be negligible on C_{ANT} estimations in this area. Therefore, the N^* correction has not

Table 2. Estimated trends on A_T, $[O_2]$, C_T , C_{ANT} and pH_T changes in two different layers of the water column defined by isopycnal layers between 1980 and 2015 based on GLODAPv2 with (column WITH) and without (column WITHOUT) OUTPACE data added. Estimated trends are obtained from slope values of a linear regression between the studied parameters and time.

	$25\,kg\,m^{-3} < \sigma_\theta < 25.5\,kg\,m^{-3}$		$27\,kg\,m^{-3} < \sigma_\theta < 27.2\,kg\,m^{-3}$	
	WITH	WITHOUT	WITH	WITHOUT
Trend on A_T in $\mu mol\,kg^{-1}\,a^{-1}$				
OUTPACE	-0.20 ± 0.07 ($n = 167$)*	-0.30 ± 0.07 ($n = 142$)*	-0.12 ± 0.07 ($n = 180$)	-0.01 ± 0.06 ($n = 174$)
MA	-0.30 ± 0.09 ($n = 85$)*	-0.47 ± 0.10 ($n = 70$)*	-0.16 ± 0.09 ($n = 99$)	-0.10 ± 0.09 ($n = 92$)
WGY	-0.20 ± 0.14 ($n = 28$)	-0.20 ± 0.19 ($n = 22$)	-0.20 ± 0.14 ($n = 35$)	-0.01 ± 0.13 ($n = 31$)
Trend on $[O_2]$ in $\mu mol\,kg^{-1}\,a^{-1}$				
OUTPACE	-0.31 ± 0.10 ($n = 167$)*	-0.61 ± 0.09 ($n = 143$)*	0.05 ± 0.11 ($n = 183$)	0.07 ± 0.10 ($n = 178$)
MA	-0.35 ± 0.16 ($n = 84$)*	-0.78 ± 0.17 ($n = 70$)*	0.06 ± 0.11 ($n = 99$)	0.04 ± 0.11 ($n = 93$)
WGY	-0.38 ± 0.11 ($n = 27$)*	-0.35 ± 0.14 ($n = 23$)*	-0.11 ± 0.30 ($n = 38$)	-0.22 ± 0.29 ($n = 34$)
Trend on C_T in $\mu mol\,kg^{-1}\,a^{-1}$				
OUTPACE	1.32 ± 0.13 ($n = 174$)*	1.63 ± 0.13 ($n = 149$)*	0.23 ± 0.13 ($n = 189$)	0.27 ± 0.11 ($n = 183$)*
MA	1.38 ± 0.21 ($n = 85$)*	1.87 ± 0.21 ($n = 70$)*	0.31 ± 0.16 ($n = 100$)	0.44 ± 0.17 ($n = 93$)*
WGY	1.57 ± 0.18 ($n = 31$)*	1.57 ± 0.23 ($n = 25$)*	0.23 ± 0.29 ($n = 40$)	0.23 ± 0.29 ($n = 36$)
Trend on C_{ANT} in $\mu mol\,kg^{-1}\,a^{-1}$				
OUTPACE	1.12 ± 0.07 ($n = 166$)*	1.25 ± 0.06 ($n = 142$)*	0.32 ± 0.05 ($n = 179$)*	0.25 ± 0.04 ($n = 174$)*
MA	1.18 ± 0.08 ($n = 84$)*	1.31 ± 0.08 ($n = 70$)*	0.40 ± 0.06 ($n = 98$)*	0.40 ± 0.06 ($n = 92$)*
WGY	1.20 ± 0.09 ($n = 28$)*	1.18 ± 0.10 ($n = 22$)*	0.13 ± 0.09 ($n = 35$)	0.11 ± 0.08 ($n = 31$)
Trend on pH_{TINSI} in a^{-1}				
OUTPACE	-0.0022 ± 0.0003 ($n = 167$)*	-0.0031 ± 0.0002 ($n = 142$)*	-0.0001 ± 0.0003 ($n = 181$)	-0.0002 ± 0.0002 ($n = 175$)
MA	-0.0022 ± 0.0004 ($n = 85$)*	-0.0033 ± 0.0004 ($n = 70$)*	-0.0004 ± 0.0003 ($n = 100$)	-0.0007 ± 0.0003 ($n = 93$)*
WGY	-0.0027 ± 0.0004 ($n = 28$)*	-0.0030 ± 0.0004 ($n = 22$)*	-0.00008 ± 0.0006 ($n = 35$)	-0.0007 ± 0.0006 ($n = 31$)

* Trend significant (p level < 0.05).

been introduced in the C_{ANT} estimates and the effect of denitrification was not quantified here.

6 Temporal changes in carbonate chemistry in the OUTPACE area

Based on the available GLODAPv2 data, temporal changes in the OUTPACE area have been assessed (Fig. 5 and Table 2). The variation in oceanic parameters with time is estimated on two isopycnal layers: a layer with $25\,kg\,m^{-3} < \sigma_\theta < 25.5\,kg\,m^{-3}$ (hereafter named $\sigma_{\theta\,25}$) and a layer with $27\,kg\,m^{-3} < \sigma_\theta < 27.2\,kg\,m^{-3}$ (hereafter named $\sigma_{\theta 27}$). These two layers correspond to the features in C_{ANT} discussed in the previous section. $\sigma_{\theta 25}$ can be considered characteristic of the upper thermocline waters (core of the salinity maximum, Fig. 2), whereas $\sigma_{\theta 27}$ can be considered characteristic of intermediate waters of southern origin (core of the salinity minimum). All the values associated with these two layers are spread between 145 and 301 dbar for $\sigma_{\theta 25}$ and between 571 and 896 dbar for $\sigma_{\theta 27}$. It must be mentioned that the study of temporal changes is based on a large sampling grid, which covers the entire OUTPACE transect (see Sect. 2.5 and Fig. 1). This could add a spatial variability that may interfere in the estimation of temporal changes.

Temporal variations in C_T and C_{ANT} between 1970 and 2015 are presented in Fig. 5. As mentioned earlier, even if C_{ANT} estimates from TrOCA are biased, a previous study by Pérez et al. (2010) suggests that the TrOCA method gives similar values to other methods for estimating C_{ANT} accumulation rates. A linear fit was applied to the observed temporal variations for A_T, $[O_2]$, C_T and C_{ANT} to check for significant trends on data collected between 1980 and 2015. The results of the performed regression analyses are presented in Table 2. Trends are evaluated with and without the data of the OUTPACE cruise in order to estimate the influence of this new dataset on the observed trends. Trends are evaluated for the entire OUTPACE area and for the MA and the WGY area. Even if presented in Fig. 5, data collected before 1980 from the GLODAPv2 database are disregarded in the estimation of the temporal trends. Indeed, for the OUTPACE area, data prior to 1980 originate from one single GEOSEC cruise in 1974, with only one measured point for $\sigma_{\theta 27}$ at WGY and no points at $\sigma_{\theta 25}$ for WGY and MA.

Table 3. Estimated depth of the $\Omega_{ara} = 1$ horizon along the OUTPACE cruise (see text for details). No values are available for stations where data up to 2000 dbar were not available (SD2 and SD13). No values were estimated for stations with $C_{ANT} < -6\,\mu mol\,kg^{-1}$.

Station	Longitude (° E)	Latitude (° N)	Depth of the $\Omega_{ara} = 1$ horizon (in m)		
			OUTPACE	Pre-ind.	Difference*
SD 1	159.9425	−17.9088	1225	NA	NA
SD 2	162.1248	−18.6078	NA	NA	NA
SD 3	165.0082	−19.4907	928	NA	NA
LD A	164.5787	−19.2233	1032	1185	153
SD 4	168.0157	−19.98	1029	1193	164
SD 5	169.9965	−21.9997	1126	1256	130
SD 6	172.1193	−21.3758	1097	1233	136
SD 7	174.2512	−20.7677	1015	1235	220
SD 8	176.364	−20.6945	1010	1171	161
SD 9	178.6087	−20.9963	1214	NA	NA
SD 11	−175.6475	−20.0057	1055	1172	117
SD 12	−172.7813	−19.5368	1013	1112	99
LD B	−170.7385	−18.1745	948	1046	98
SD13	−169.0728	−18.2007	NA	NA	NA
LD C	−165.7792	−18.4842	854	941	87
SD 14	−162.9992	−18.3952	889	1006	117
SD 15	−159.9913	−18.2618	917	1043	126

* Difference (in m) between the depth of the $\Omega_{ara} = 1$ horizon at the pre-industrial period and the OUTPACE cruise. NA – not available.

At $\sigma_{\theta 25}$, a significant decrease in A_T of $-0.20 \pm 0.07\,\mu mol\,kg^{-1}\,a^{-1}$ is observed over the entire OUTPACE area. A decrease of $-0.30 \pm 0.09\,\mu mol\,kg^{-1}\,a^{-1}$ is also observed in the MA area, whereas no significant trend is observed for the WGY area. However, when A_T is normalized to salinity, no significant trends are observed in $A_{T\,n35}$ suggesting that the observed trend in A_T can be attributed to salinity changes rather than changes in calcification. Significant negative trends are observed for $[O_2]$ over the entire area ($-0.31 \pm 0.10\,\mu mol\,kg^{-1}\,a^{-1}$), in MA ($-0.35 \pm 0.16\,\mu mol\,kg^{-1}\,a^{-1}$) and in WGY ($-0.38 \pm 0.11\,\mu mol\,kg^{-1}\,a^{-1}$). The decrease in $[O_2]$ which corresponds to a positive trend in AOU suggested an increase in the remineralization of organic matter at $\sigma_{\theta 25}$. Significant increasing trends were observed for C_T over the entire area ($+1.32 \pm 0.13\,\mu mol\,kg^{-1}\,a^{-1}$), in MA ($+1.38 \pm 0.21\,\mu mol\,kg^{-1}\,a^{-1}$) and in WGY ($+1.57 \pm 0.13\,\mu mol\,kg^{-1}\,a^{-1}$). For C_{ANT}, the trends were slightly slower ($+1.12 \pm 0.07$ to $+1.2 \pm 0.09\,\mu mol\,kg^{-1}\,a^{-1}$) and not significantly different between MA and WGY. Taking into account the OUTPACE dataset does not change the overall significance of the observed trends and only minor changes (mostly within the error of the estimates) are observed. If we assume a C_T increase of 0.5 to $1\,\mu mol\,kg^{-1}\,a^{-1}$ (depending on the buffer factors considered) associated with the recent rise in atmospheric CO_2 (see for example Murata et al., 2007), the C_T increase in the OUTPACE area is faster than thermodynamics would govern, whereas the C_{ANT} is closer to this thermodynamic value. The higher increase in C_T could be related to an increase in remineralization processes as deduced from $[O_2]$ trends, with an overall consistency between the rate of C_T increase and the rate of decrease in $[O_2]$. However, the important increase in C_{ANT} observed between 2005 and 2015 between 10 and 30° S on the P16 line (at the eastern side of the OUTPACE transect) by Carter et al. (2017) is not supported by significant differences in the trends of C_{ANT} observed between MA and WGY in this study.

At $\sigma_{\theta 27}$, the only significant trend observed is an increase in C_{ANT} of ca. $0.40 \pm 0.06\,\mu mol\,kg^{-1}\,a^{-1}$ in the MA area. When the OUTPACE dataset is not considered, a similar trend is observed for C_T in the MA area. This trend is compatible with the observed increase in C_{ANT} by Kouketsu et al. (2013) along the P21 line close to the isopycnal layer $27\,kg\,m^{-3}$. As this increase is not observed in WGY and if we assume that the $\sigma_{\theta 27}$ is filed with AAIWs, this suggest that the accumulation of C_{ANT} in AAIW is faster west of the 170° W line than to the east, but no clear explanation for this trend can be given.

7 Towards an enhanced "ocean acidification" in the WTSP?

Temporal variations in pH_T between 1970 and 2015 are presented in Fig. 5c and f with rates of pH_T decrease of $-0.0022 \pm 0.0004\,a^{-1}$ for MA and $-0.0027 \pm 0.0004\,a^{-1}$ for WGY at $\sigma_{\theta 25}$ (Table 2) between 1980 and 2015. Based on the C_{ANT} rates estimated in the previous section (1.1 to $1.2\,\mu mol\,kg^{-1}\,a^{-1}$) and based on a constant value of A_T of

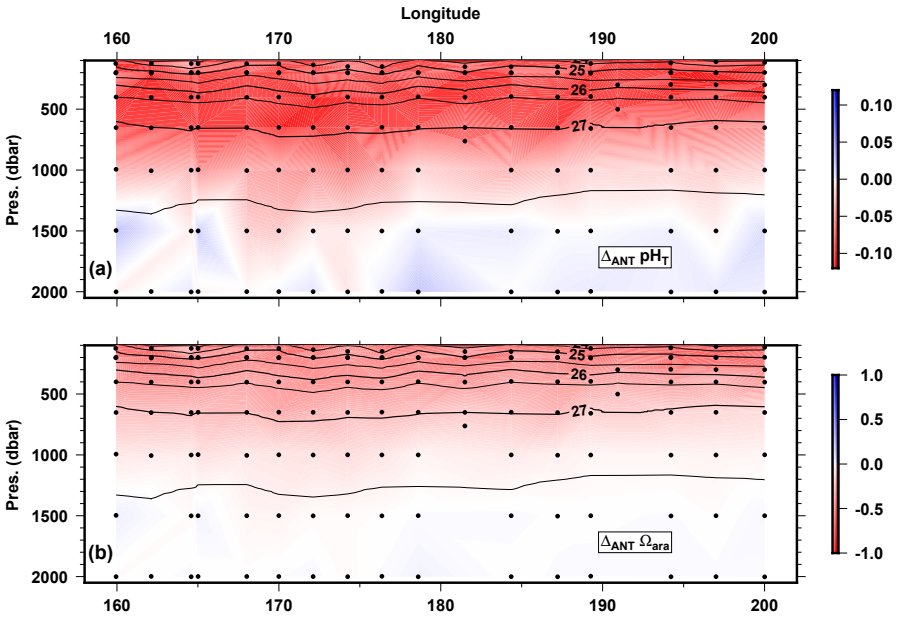

Figure 6. Longitudinal variations in **(a)** pH_T changes and **(b)** Ω_{ara} changes between the pre-industrial period and the present time along the OUTPACE transect between 100 and 2000 dbar depth (see text for details). Black contour lines represent the isopycnal horizons based on potential density referenced to a pressure of 0 dbar.

2285 µmol kg^{-1} (mean value of $A_{T\,n35}$ on $\sigma_{\theta 25}$) and a constant temperature of 20 °C (mean value of temperature on $\sigma_{\theta 25}$), we can estimate a pH_T decrease rate of −0.0023 to −0.0025 a^{-1}. This indicates that rates of oceanic pH_T decrease (ocean acidification) can mostly be explained by the increase in C_{ANT}. These rates of acidification are higher than the values reported by Waters et al. (2011) in the western South Pacific along the P06 Line (south of OUTPACE area at 32° S) between two visits in 1992 and 2008. They are also higher than the surface rates of pH_T decrease of -0.0016 ± 0.0001 a^{-1} recorded at the HOT station in the tropical North Pacific and of -0.0017 ± 0.0001 and -0.0018 ± 0.0001 a^{-1} in the tropical North Atlantic at BATS and ESTOC stations, respectively (Bates et al., 2014). However, differences in buffer factors between the surface and subsurface can partially explain these differences. Nevertheless, our results in the subsurface ($\sigma_{\theta 25}$) based on GLODAPv2 and OUTPACE data (C_T and A_T) are similar to pH_T trends derived from fCO_2 surface observations (e.g., Lauvset et al., 2015). In the southern subtropical and equatorial Pacific regions, using SOCAT version2, Lauvset et al. (2015) evaluate contrasting fCO_2 and pH_T trends, ranging between +1.1 and +3.5 µatm a^{-1} for fCO_2 and between −0.001 and −0.0023 a^{-1} for pH_T. If we revisit these estimates, using surface fCO_2 observations available in the OUTPACE region (18–22° S/170–200° E) in SOCAT version 6 (Bakker et al., 2016; http://www.socat.info, last access: 10 August 2018) and assuming a constant alkalinity (2300 µmol kg^{-1}, average of surface data), we can calculate pH_T and C_T from fCO_2 and temperature data. The resulting long-term trends for the period 1980–2016 for fCO_2, C_T and pH_T are, respectively, $+1.27 \pm 0.01$ µatm a^{-1}, $+1.03 \pm 0.01$ µmol kg^{-1} a^{-1} and -0.0013 ± 0.0001 a^{-1}. Interestingly, for the period 2000–2016 the trends are $+2.53 \pm 0.02$ µatm a^{-1}, $+2.02 \pm 0.02$ µmol kg^{-1} a^{-1} and -0.0025 ± 0.0003 a^{-1}, suggesting an acceleration of the signals in recent years. These results, based on fCO_2 observations in surface waters, confirm the trends we detected for C_T and pH_T in subsurface layers ($\sigma_{\theta 25}$).

In Fig. 6, estimates of the so-called "anthropogenic pH_T change" ($\Delta_{ANT}pH_T$) and "anthropogenic Ω_{ara} change" ($\Delta_{ANT}\Omega_{ara}$), which correspond to the difference in pH_T and Ω_{ara} between the time of the OUTPACE cruise (modern time) and the pre-industrial period, are presented. The pH_T and Ω_{ara} correspond to the values presented in Fig. 3, whereas the pre-industrial values corresponds to pH_T and Ω_{ara} estimated with C_T minus C_{ANT}. All other parameters (temperature, salinity, alkalinity and nutrients) are assumed to remain constant over time. The main features for the distribution of $\Delta_{ANT}pH_T$ and $\Delta_{ANT}\Omega_{ara}$ logically reflect the distribution of the estimated C_{ANT} in this study because C_{ANT} is the only driving force in these estimations. The estimated pH_T decrease reaches values slightly higher than 0.1 and the estimated Ω_{ara} decrease reaches values of 0.75 since the pre-industrial period for areas with the highest C_{ANT} accumulation. When considering an error in C_{ANT} of 6 µmol kg^{-1}, we can assume that we are able to distinguish changes of 0.0012 for pH_T and 0.06 for Ω_{ara}. Decreases in pH_T and Ω_{ara} are

thus detectable below 1000 dbar in the MA waters and above 1000 dbar in WGY waters.

A decrease in pH_T of 0.1 units since the pre-industrial period is a generally accepted value for oceanic waters affected by C_{ANT} penetration (e.g., Royal Society , Great Britain). Several studies have assessed the rate of ocean acidification based on successive visits to different oceanic areas. For the South Pacific Ocean, Carter et al. (2017) reports decreases in oceanic pH_T since the pre-industrial period of −0.09 and −0.11 pH_T units for the latitude band from 10 to 20° S and from 20 to 30° S, respectively, along the P16 line (150° W) situated on the eastern side of the OUTPACE area. These are in good agreement with our estimates in this area.

Based on an interpolation of the estimated Ω_{ara} during OUTPACE and the pre-industrial Ω_{ara}, we calculated the depth of the horizon where $\Omega_{ara} = 1$ for the different stations of the OUTPACE transect (Table 3) in 2015 and the pre-industrial period based on the $\Delta_{ANT}\Omega_{ara}$ estimates. We observed an upward migration of the aragonite saturation horizon of up to 220 m in the MA area along the OUTPACE transect (Table 3). This upward migration of the $\Omega_{ara} = 1$ horizon is higher than the migration of 30 to 100 m observed between the 1990s and the pre-industrial period in early studies (Feely et al., 2004) in the Pacific based on the WOCE dataset illustrating the continuous acidification of the WTSP.

8 Conclusions

Based on A_T and C_T data and related properties collected during the OUTPACE cruise, we estimated different parameters of the carbonate system along a longitudinal section of nearly 4000 km and up to 2000 dbar in WTSP. Even if the vertical and horizontal resolution is low compared to the WOCE lines and precludes a rigorous comparison with this high-quality dataset, we estimated that the measured carbonate chemistry parameters are in good agreement with previous data collected in this area. Based on the estimation of C_{ANT} from the TrOCA method, we find C_{ANT} penetration in the WTSP and impacts on pH_T and saturation state of calcium carbonate since the pre-industrial period that are in good agreement with previous observations in this area. As mentioned above, C_{ANT} values from TrOCA estimates are not reliable in surface layer. However, based on GLODAPv2 and the SOCAT database, our estimation of C_{ANT} in the subsurface seems to be in good agreement with expected changes in surface waters. The enhanced impact of ocean acidification in the subtropical South Pacific suggested by our study highlights the necessity of sustained research efforts in this largely underexplored part of the world ocean. The presented dataset collected along the OUTPACE transect could complement existing sections visited nearly every decade in the South Pacific Ocean and in particular the P21 line, which was last visited in 2009.

Data availability. OUTPACE cruise data are available at the French INSU/CNRS LEFE CYBER database (scientific coordinator: Hervé Claustre; data manager and webmaster: Catherine Schmechtig) at the following web address: http://www.obs-vlfr.fr/proof/php/outpace/outpace.php (last access: 10 August 2018). GLODAPv2 data are available at the following web address: https://www.glodap.info/ (last access: 10 August 2018). SOCAT version 6 data are available at the following web address: https://www.socat.info/ (last access: 10 August 2018).

Competing interests. The authors declare that they have no conflict of interest.

Special issue statement. This article is part of the special issue "Interactions between planktonic organisms and biogeochemical cycles across trophic and N_2 fixation gradients in the western tropical South Pacific Ocean: a multidisciplinary approach (OUTPACE experiment)". It is not associated with a conference.

Acknowledgements. This is a contribution of the OUTPACE (Oligotrophy from Ultra-oligoTrophy PACific Experiment) project (https://outpace.mio.univ-amu.fr/, last access: 10 August 2018) funded by the French national research agency (ANR-14-CE01-0007-01), the LEFE-CyBER program (CNRS-INSU), the GOPS program (IRD) and the CNES (BC T23, ZBC 4500048836). The OUTPACE cruise (https://doi.org/10.17600/15000900) was managed by the MIO (OSU Institut Pytheas, AMU) from Marseille (France), which has received funding from the European FEDER Fund under project 1166-39417. The SNAPO-CO_2 service at LOCEAN is supported by CNRS-INSU and OSU Ecce-Terra. The Surface Ocean CO_2 Atlas (SOCAT) is an international effort, endorsed by the International Ocean Carbon Coordination Project (IOCCP), the Surface Ocean Lower Atmosphere Study (SOLAS) and the Integrated Marine Biosphere Research (IMBeR) program, to deliver a uniformly quality-controlled surface ocean CO_2 database. The many researchers and funding agencies responsible for the collection of data and quality control are thanked for their contributions to SOCAT. The authors thank the crew of the R/V *L'Atalante* for outstanding shipboard operation. Catherine Schmechtig is warmly thanked for the LEFE CYBER database management. Aurelia Lozingot is acknowledged for the administrative work. Pierre Marrec is thanked for his insightful comments on the present work. The two anonymous referees are thanked for helping improve a previous version of this paper. The authors acknowledge the assistance of the editorial staff of *Biogeosciences*.

Edited by: Emilio Marañón
Reviewed by: two anonymous referees

References

Álvarez, M., Lo Monaco, C., Tanhua, T., Yool, A., Oschlies, A., Bullister, J. L., Goyet, C., Metzl, N., Touratier, F., McDonagh, E., and Bryden, H. L.: Estimating the storage of anthro-

pogenic carbon in the subtropical Indian Ocean: a comparison of five different approaches, Biogeosciences, 6, 681–703, https://doi.org/10.5194/bg-6-681-2009, 2009.

Azouzi, L., Goyet, C., Gonçalves Ito, R., and Touratier, F.: Corrigendum to "Anthropogenic carbon distribution in the eastern South Pacific Ocean" published in Biogeosciences, 6, 149–156, 2009, Biogeosciences, 6, 361–361, https://doi.org/10.5194/bg-6-361-2009, 2009.

Bakker, D. C. E., Pfeil, B., Landa, C. S., Metzl, N., O'Brien, K. M., Olsen, A., Smith, K., Cosca, C., Harasawa, S., Jones, S. D., Nakaoka, S.-I., Nojiri, Y., Schuster, U., Steinhoff, T., Sweeney, C., Takahashi, T., Tilbrook, B., Wada, C., Wanninkhof, R., Alin, S. R., Balestrini, C. F., Barbero, L., Bates, N. R., Bianchi, A. A., Bonou, F., Boutin, J., Bozec, Y., Burger, E. F., Cai, W.-J., Castle, R. D., Chen, L., Chierici, M., Currie, K., Evans, W., Featherstone, C., Feely, R. A., Fransson, A., Goyet, C., Greenwood, N., Gregor, L., Hankin, S., Hardman-Mountford, N. J., Harlay, J., Hauck, J., Hoppema, M., Humphreys, M. P., Hunt, C. W., Huss, B., Ibánhez, J. S. P., Johannessen, T., Keeling, R., Kitidis, V., Körtzinger, A., Kozyr, A., Krasakopoulou, E., Kuwata, A., Landschützer, P., Lauvset, S. K., Lefèvre, N., Lo Monaco, C., Manke, A., Mathis, J. T., Merlivat, L., Millero, F. J., Monteiro, P. M. S., Munro, D. R., Murata, A., Newberger, T., Omar, A. M., Ono, T., Paterson, K., Pearce, D., Pierrot, D., Robbins, L. L., Saito, S., Salisbury, J., Schlitzer, R., Schneider, B., Schweitzer, R., Sieger, R., Skjelvan, I., Sullivan, K. F., Sutherland, S. C., Sutton, A. J., Tadokoro, K., Telszewski, M., Tuma, M., van Heuven, S. M. A. C., Vandemark, D., Ward, B., Watson, A. J., and Xu, S.: A multidecade record of high-quality fCO_2 data in version 3 of the Surface Ocean CO_2 Atlas (SOCAT), Earth Syst. Sci. Data, 8, 383–413, https://doi.org/10.5194/essd-8-383-2016, 2016.

Bates, N., Astor, Y., Church, M., Currie, K., Dore, J., González-Dávila, M., Lorenzoni, L., Muller-Karger, F., Olafsson, J., and Santa-Casiano, M.: A Time-Series View of Changing Ocean Chemistry Due to Ocean Uptake of Anthropogenic CO_2 and Ocean Acidification, Oceanography, 27, 126–141, https://doi.org/10.5670/oceanog.2014.16, 2014.

Bonnet, S., Caffin, M., Berthelot, H., and Moutin, T.: Hot spot of N_2 fixation in the western tropical South Pacific pleads for a spatial decoupling between N_2 fixation and denitrification, P. Natl. Acad. Sci. USA, 114, E2800–E2801, https://doi.org/10.1073/pnas.1619514114, 2017.

Carter, B. R., Feely, R. A., Mecking, S., Cross, J. N., Macdonald, A. M., Siedlecki, S. A., Talley, L. D., Sabine, C. L., Millero, F. J., Swift, J. H., Dickson, A. G., and Rodgers, K. B.: Two decades of Pacific anthropogenic carbon storage and ocean acidification along Global Ocean Ship-based Hydrographic Investigations Program sections P16 and P02: Decadal Pacific C_{anth} Changes by EMLR, Global Biogeochem. Cy., 31, 306–327, https://doi.org/10.1002/2016GB005485, 2017.

de Verneil, A., Rousselet, L., Doglioli, A. M., Petrenko, A. A., and Moutin, T.: The fate of a southwest Pacific bloom: gauging the impact of submesoscale vs. mesoscale circulation on biological gradients in the subtropics, Biogeosciences, 14, 3471–3486, https://doi.org/10.5194/bg-14-3471-2017, 2017.

DeVries, T., Holzer, M., and Primeau, F.: Recent increase in oceanic carbon uptake driven by weaker upper-ocean overturning, Nature, 542, 215–218, https://doi.org/10.1038/nature21068, 2017.

Dickson, A.: An exact definition of total alkalinity and a procedure for the estimation of alkalinity and total inorganic carbon from titration data, Deep-Sea Res. Pt. A, 28, 609–623, https://doi.org/10.1016/0198-0149(81)90121-7, 1981.

Dickson, A.: Standards for Ocean Measurements, Oceanography, 23, 34–47, https://doi.org/10.5670/oceanog.2010.22, 2010.

Dickson, A. and Goyet, C. (Eds.): Handbook of methods for the analysis of the various parameters of the carbon dioxide system in sea water, version 2, no. 74 in ORNL/CDIAC-74, US Departement of Energy, 1994.

Dickson, A. G.: Standard potential of the reaction: $AgCl(s) + 12H_2(g) = Ag(s) + HCl(aq)$, and and the standard acidity constant of the ion HSO_4^- in synthetic sea water from 273.15 to 318.15 K, J. Chem. Thermodyn., 22, 113–127, https://doi.org/10.1016/0021-9614(90)90074-Z, 1990.

Dickson, A. G., Sabine, C. L., Christian, J. R., Bargeron, C. P., and North Pacific Marine Science Organization (Eds.): Guide to best practices for ocean CO_2 measurements, no. 3 in PICES special publication, North Pacific Marine Science Organization, Sidney, BC, 2007.

Edmond, J. M.: High precision determination of titration alkalinity and total carbon dioxide content of sea water by potentiometric titration, Deep-Sea Research and Oceanographic Abstracts, 17, 737–750, https://doi.org/10.1016/0011-7471(70)90038-0, 1970.

Feely, R. A., Sabine, C. L., Lee, K., Berelson, W., Kleypas, J., Fabry, V. J., and Millero, F. J: Impact of Anthropogenic CO_2 on the $CaCO_3$ System in the Oceans, Science, 305, 362–366, https://doi.org/10.1126/science.1097329, 2004.

Fumenia, A., Moutin, T., Bonnet, S., Benavides, M., Petrenko, A., Helias Nunige, S., and Maes, C.: Excess nitrogen as a marker of intense dinitrogen fixation in the Western Tropical South Pacific Ocean: impact on the thermocline waters of the South Pacific, Biogeosciences Discuss., https://doi.org/10.5194/bg-2017-557, in review, 2018.

Ganachaud, A., Cravatte, S., Sprintall, J., Germineaud, C., Alberty, M., Jeandel, C., Eldin, G., Metzl, N., Bonnet, S., Benavides, M., Heimburger, L.-E., Lefèvre, J., Michael, S., Resing, J., Quéroué, F., Sarthou, G., Rodier, M., Berthelot, H., Baurand, F., Grelet, J., Hasegawa, T., Kessler, W., Kilepak, M., Lacan, F., Privat, E., Send, U., Van Beek, P., Souhaut, M., and Sonke, J. E.: The Solomon Sea: its circulation, chemistry, geochemistry and biology explored during two oceanographic cruises, Elem. Sci. Anth., 5, 33, https://doi.org/10.1525/elementa.221, 2017.

Garcia, H. E. and Gordon, L. I.: Oxygen solubility in seawater: Better fitting equations, Limnol. Oceanogr., 37, 1307–1312, https://doi.org/10.4319/lo.1992.37.6.1307, 1992.

Gattuso, J.-P. and Lavigne, H.: Technical Note: Approaches and software tools to investigate the impact of ocean acidification, Biogeosciences, 6, 2121–2133, https://doi.org/10.5194/bg-6-2121-2009, 2009.

Gruber, N. and Sarmiento, J. L.: Global patterns of marine nitrogen fixation and denitrification, Global Biogeochem. Cy., 11, 235–266, https://doi.org/10.1029/97GB00077, 1997.

Hartin, C. A., Fine, R. A., Sloyan, B. M., Talley, L. D., Chereskin, T. K., and Happell, J.: Formation rates of Subantarctic mode water and Antarctic intermediate water within the South Pacific, Deep-Sea Res. Pt. I, 58, 524–534, https://doi.org/10.1016/j.dsr.2011.02.010, 2011.

Key, R. M., Kozyr, A., Sabine, C. L., Lee, K., Wanninkhof, R., Bullister, J. L., Feely, R. A., Millero, F. J., Mordy, C., and Peng, T.-H.: A global ocean carbon climatology: Results from Global Data Analysis Project (GLODAP): GLOBAL OCEAN CARBON CLIMATOLOGY, Global Biogeochem. Cy., 18, GB4031, https://doi.org/10.1029/2004GB002247, 2004.

Key, R., Olsen, A., Van Heuven, S., Lauvset, S., Velo, A., Lin, X., Schirnick, C., Kozyr, A., Tanhua, T., Hoppema, M., Jutterstrom, S., Steinfeldt, R., Jeansson, E., Ishi, M., Perez, F., and Suzuki, T.: Global Ocean Data Analysis Project, Version 2 (GLODAPv2), ORNL/CDIAC-162, ND-P093, dataset, https://doi.org/10.3334/CDIAC/OTG.NDP093_GLODAPv2, 2015.

Kouketsu, S., Murata, A., and Doi, T.: Decadal changes in dissolved inorganic carbon in the Pacific Ocean: DIC changes in the pacific, Global Biogeochem. Cy., 27, 65–76, https://doi.org/10.1029/2012GB004413, 2013.

Langdon, C.: Determination of Dissolved Oxygen in Seawater by Winkler Titration Using the Amperometric Technique, no. 14 in IOCCP Report, ICPO Publication, available at: http://www.go-ship.org/HydroMan.html (last access: 10 August 2018), 2010.

Lauvset, S. K., Gruber, N., Landschützer, P., Olsen, A., and Tjiputra, J.: Trends and drivers in global surface ocean pH over the past 3 decades, Biogeosciences, 12, 1285–1298, https://doi.org/10.5194/bg-12-1285-2015, 2015.

Le Quéré, C., Andrew, R. M., Friedlingstein, P., Sitch, S., Pongratz, J., Manning, A. C., Korsbakken, J. I., Peters, G. P., Canadell, J. G., Jackson, R. B., Boden, T. A., Tans, P. P., Andrews, O. D., Arora, V. K., Bakker, D. C. E., Barbero, L., Becker, M., Betts, R. A., Bopp, L., Chevallier, F., Chini, L. P., Ciais, P., Cosca, C. E., Cross, J., Currie, K., Gasser, T., Harris, I., Hauck, J., Haverd, V., Houghton, R. A., Hunt, C. W., Hurtt, G., Ilyina, T., Jain, A. K., Kato, E., Kautz, M., Keeling, R. F., Klein Goldewijk, K., Körtzinger, A., Landschützer, P., Lefèvre, N., Lenton, A., Lienert, S., Lima, I., Lombardozzi, D., Metzl, N., Millero, F., Monteiro, P. M. S., Munro, D. R., Nabel, J. E. M. S., Nakaoka, S.-I., Nojiri, Y., Padin, X. A., Peregon, A., Pfeil, B., Pierrot, D., Poulter, B., Rehder, G., Reimer, J., Rödenbeck, C., Schwinger, J., Séférian, R., Skjelvan, I., Stocker, B. D., Tian, H., Tilbrook, B., Tubiello, F. N., van der Laan-Luijkx, I. T., van der Werf, G. R., van Heuven, S., Viovy, N., Vuichard, N., Walker, A. P., Watson, A. J., Wiltshire, A. J., Zaehle, S., and Zhu, D.: Global Carbon Budget 2017, Earth Syst. Sci. Data, 10, 405–448, https://doi.org/10.5194/essd-10-405-2018, 2018.

Lo Monaco, C., Goyet, C., Metzl, N., Poisson, A., and Touratier, F.: Distribution and inventory of anthropogenic CO_2 in the Southern Ocean: Comparison of three data-based methods, J. Geophys. Res., 110, C09S02, https://doi.org/10.1029/2004JC002571, 2005.

Lueker, T. J., Dickson, A. G., and Keeling, C. D.: Ocean pCO_2 calculated from dissolved inorganic carbon, alkalinity, and equations for K_1 and K_2: validation based on laboratory measurements of CO_2 in gas and seawater at equilibrium, Mar. Chem., 70, 105–119, https://doi.org/10.1016/S0304-4203(00)00022-0, 2000.

Moutin, T., Doglioli, A. M., de Verneil, A., and Bonnet, S.: Preface: The Oligotrophy to the UlTra-oligotrophy PACific Experiment (OUTPACE cruise, 18 February to 3 April 2015), Biogeosciences, 14, 3207–3220, https://doi.org/10.5194/bg-14-3207-2017, 2017.

Moutin, T., Wagener, T., Caffin, M., Fumenia, A., Gimenez, A., Baklouti, M., Bouruet-Aubertot, P., Pujo-Pay, M., Leblanc, K., Lefevre, D., Helias Nunige, S., Leblond, N., Grosso, O., and de Verneil, A.: Nutrient availability and the ultimate control of the biological carbon pump in the western tropical South Pacific Ocean, Biogeosciences, 15, 2961–2989, https://doi.org/10.5194/bg-15-2961-2018, 2018.

Murata, A., Kumamoto, Y., Watanabe, S., and Fukasawa, M.: Decadal increases of anthropogenic CO_2 in the South Pacific subtropical ocean along 32° S, J. Geophys. Res., 112, C05033, https://doi.org/10.1029/2005JC003405, 2007.

Murata, A., Hayashi, K., Kumamoto, Y., and Sasaki, K.-I.: Detecting the progression of ocean acidification from the saturation state of $CaCO_3$ in the subtropical South Pacific, Global Biogeochem. Cy., 29, 463–475, https://doi.org/10.1002/2014GB004908, 2015.

Olsen, A., Key, R. M., van Heuven, S., Lauvset, S. K., Velo, A., Lin, X., Schirnick, C., Kozyr, A., Tanhua, T., Hoppema, M., Jutterström, S., Steinfeldt, R., Jeansson, E., Ishii, M., Pérez, F. F., and Suzuki, T.: The Global Ocean Data Analysis Project version 2 (GLODAPv2) – an internally consistent data product for the world ocean, Earth Syst. Sci. Data, 8, 297–323, https://doi.org/10.5194/essd-8-297-2016, 2016.

Oudot, C., Gerard, R., Morin, P., and Gningue, I.: Precise shipboard determination of dissolved oxygen (Winkler procedure) for productivity studies with a commercial system1, Limnol. Oceanogr., 33, 146–150, https://doi.org/10.4319/lo.1988.33.1.0146, 1988.

Owens, W. B. and Millard, R. C.: A New Algorithm for CTD Oxygen Calibration, J. Phys. Oceanogr., 15, 621–631, https://doi.org/10.1175/1520-0485(1985)015<0621:ANAFCO>2.0.CO;2, 1985.

Pérez, F. F. and Fraga, F.: A precise and rapid analytical procedure for alkalinity determination, Mar. Chem., 21, 169–182, https://doi.org/10.1016/0304-4203(87)90037-5, 1987.

Pérez, F. F., Vázquez-Rodríguez, M., Mercier, H., Velo, A., Lherminier, P., and Ríos, A. F.: Trends of anthropogenic CO_2 storage in North Atlantic water masses, Biogeosciences, 7, 1789–1807, https://doi.org/10.5194/bg-7-1789-2010, 2010.

Riebesell, U., Zondervan, I., Rost, B., Tortell, P. D., Zeebe, R. E., and Morel, F. M. M.: Reduced calcification of marine plankton in response to increased atmospheric CO_2, Nature, 407, 364–367, https://doi.org/10.1038/35030078, 2000.

Royal Society (Great Britain): Ocean acidification due to increasing atmospheric carbon dioxide, Royal Society, London, oCLC: 60805277, available at: https://royalsociety.org/topics-policy/publications/2005/ocean-acidification/ (last access: 10 August 2018), 2005.

Sabine, C. L. and Tanhua, T.: Estimation of Anthropogenic CO_2 Inventories in the Ocean, Annu. Rev. Mar. Sci., 2, 175–198, https://doi.org/10.1146/annurev-marine-120308-080947, 2010.

Sabine, C. L., Feely, R. A., Gruber, N., Key, R. M., Lee, K., Bullister, J. L., Wanninkhof, R., Wong, C. S., Wallace, D. W. R., Tilbrook, B., Millero, F. J., Peng, T.-H., Kozyr, A., Ono, T., and Rios, A. F.: The Oceanic Sink for Anthropogenic CO_2, Science, 305, 367–371, https://doi.org/10.1126/science.1097403, 2004.

Sabine, C. L., Feely, R. A., Millero, F. J., Dickson, A. G., Langdon, C., Mecking, S., and Greeley, D.: Decadal

changes in Pacific carbon, J. Geophys. Res., 113, C07021, https://doi.org/10.1029/2007JC004577, 2008.

Takahashi, T., Sutherland, S., Chipman, D., Goddard, J., Ho, C., Newberger, T., Sweeney, C., and Munro, D.: Climatological distributions of pH, pCO_2, total CO_2, alkalinity, and $CaCO_3$ saturation in the global surface ocean, and temporal changes at selected locations, Mar. Chem., 164, 95–125, https://doi.org/10.1016/j.marchem.2014.06.004, 2014.

Tomczak, M. and Godfrey, J. S.: Regional oceanography: an introduction, 2nd Edn., Daya Publ. House, Delhi, 2003.

Touratier, F. and Goyet, C.: Applying the new TrOCA approach to assess the distribution of anthropogenic CO_2 in the Atlantic Ocean, J. Marine Syst., 46, 181–197, https://doi.org/10.1016/j.jmarsys.2003.11.020, 2004a.

Touratier, F. and Goyet, C.: Definition, properties, and Atlantic Ocean distribution of the new tracer TrOCA, J. Marine Syst., 46, 169–179, https://doi.org/10.1016/j.jmarsys.2003.11.016, 2004b.

Touratier, F., Azouzi, L., and Goyet, C.: CFC-11, $\Delta^{14}C$ and ^{3}H tracers as a means to assess anthropogenic CO_2 concentrations in the ocean, Tellus B, 59, 318–325, https://doi.org/10.1111/j.1600-0889.2006.00247.x, 2007.

Valladares, J., Fennel, W., and Morozov, E.: Replacement of EOS – 80 with the International Thermodynamic Equation of Seawater – 2010 (TEOS–10), Deep-Sea Res. Pt. I, 58, p. 978, https://doi.org/10.1016/j.dsr.2011.07.005, 2011.

Vázquez-Rodríguez, M., Touratier, F., Lo Monaco, C., Waugh, D. W., Padin, X. A., Bellerby, R. G. J., Goyet, C., Metzl, N., Ríos, A. F., and Pérez, F. F.: Anthropogenic carbon distributions in the Atlantic Ocean: data-based estimates from the Arctic to the Antarctic, Biogeosciences, 6, 439–451, https://doi.org/10.5194/bg-6-439-2009, 2009.

Waters, J. F., Millero, F. J., and Sabine, C. L.: Changes in South Pacific anthropogenic carbon, Global Biogeochem. Cy., 25, GB4011, https://doi.org/10.1029/2010GB003988, 2011.

Winkler, L. W.: Die Bestimmung des im Wasser gelösten Sauerstoffes, Ber. Dtsch. Chem. Ges., 21, 2843–2854, https://doi.org/10.1002/cber.188802102122, 1888.

Yool, A., Oschlies, A., Nurser, A. J. G., and Gruber, N.: A model-based assessment of the TrOCA approach for estimating anthropogenic carbon in the ocean, Biogeosciences, 7, 723–751, https://doi.org/10.5194/bg-7-723-2010, 2010.

Yoshikawa, C., Makabe, A., Shiozaki, T., Toyoda, S., Yoshida, O., Furuya, K., and Yoshida, N.: Nitrogen isotope ratios of nitrate and N^* anomalies in the subtropical South Pacific, Geochem. Geophy. Geosy., 16, 1439–1448, https://doi.org/10.1002/2014GC005678, 2015.